HHS Public Access

Author manuscript

Cancer Immunol Res. Author manuscript; available in PMC 2022 January 01.

Published in final edited form as:

Cancer Immunol Res. 2021 January ; 9(1): 62–74. doi:10.1158/2326-6066.CIR-20-0253.

CD28 Costimulatory Domain–Targeted Mutations Enhance Chimeric Antigen Receptor T-cell Function

Justin C. Boucher[1], **Gongbo Li**[1], **Hiroshi Kotani**[1], **Maria L. Cabral**[2], **Dylan Morrissey**[3], **Sae Bom Lee**[1,4], **Kristen Spitler**[1], **Nolan J. Beatty**[1,4], **Estelle V. Cervantes**[3], **Bishwas Shrestha**[1], **Bin Yu**[1], **Aslamuzzaman Kazi**[5], **Xuefeng Wang**[6], **Said M. Sebti**[5], **Marco L. Davila**[1,3]

[1]Department of Blood and Marrow Transplant and Cellular Immunotherapy, Division of Clinical Science, H. Lee Moffitt Cancer Center, Tampa, Florida.

[2]Department of Cell Biology, Microbiology, and Molecular Biology, College of Arts and Sciences, University of South Florida, Tampa, Florida.

[3]Morsani College of Medicine, University of South Florida Health, Tampa, Florida.

[4]Cancer Biology Ph.D. Program, University of South Florida, Tampa, Florida.

[5]Drug Discovery Program, H. Lee Moffitt Cancer Center, Tampa, Florida.

[6]Department of Biostatistics and Bioinformatics, H. Lee Moffitt Cancer Center, Tampa, Florida.

Abstract

An obstacle to the development of chimeric antigen receptor (CAR) T cells is the limited understanding of CAR T-cell biology and the mechanisms behind their antitumor activity. We and others have shown that CARs with a CD28 costimulatory domain drive high T-cell activation, which leads to exhaustion and shortened persistence. This work led us to hypothesize that by

Corresponding Author: Marco L. Davila, H. Lee Moffitt Cancer Center, 12902 Magnolia Drive, FOB-3, Tampa, FL 33612. Phone: 813-745-7202; marco.davila@moffitt.org.

Authors' Disclosures

K. Spitler reports grants, nonfinancial support, and other from Atara Pharmaceuticals during the conduct of the study. E.V. Cervantes reports grants from Atara during the conduct of the study. S.M. Sebti reports personal fees from Prescient Therapeutics outside the submitted work. M.L. Davila reports grants and personal fees from Atara Biotherapeutics (licensing fees) during the conduct of the study; grants from Novartis, personal fees from Precision Biosciences and Bellicum, and other from Adaptive Biotechnologies (stock), Bluebird Bio (stock), and Allogene (stock) outside the submitted work; and a patent for CD28-targeted mutation licensed. No disclosures were reported by the other authors.

Current address for H. Kotani: Oncology Clinical Research Department, Takeda Pharmaceutical Company Limited, Osaka, Japan; current address for M.L. Cabral: Bluebird Bio Inc., Cambridge, Massachusetts; and current address for S.M. Sebti: Department of Pharmacology and Toxicology at the VCU School of Medicine, Richmond, Virginia.

Authors' Contributions

J.C. Boucher: Conceptualization, formal analysis, validation, investigation, methodology, writing–original draft, writing–review and editing. **G. Li:** Investigation, writing–review and editing. **H. Kotani:** Investigation, writing–review and editing. **M.L. Cabral:** Investigation, writing–review and editing. **D. Morrissey:** Investigation, writing–review and editing. **S.B. Lee:** Investigation, writing–review and editing. **K. Spitler:** Investigation, writing–review and editing. **N.J. Beatty:** Investigation, writing–review and editing. **E.V. Cervantes:** Investigation, writing–review and editing. **B. Shrestha:** Investigation, writing–review and editing. **B. Yu:** Investigation, writing–review and editing. **A. Kazi:** Validation, investigation, writing–review and editing. **X. Wang:** Data curation, formal analysis, writing–review and editing. **SM. Sebti:** Formal analysis, validation, writing–review and editing. **M.L. Davila:** Conceptualization, formal analysis, supervision, funding acquisition, writing–original draft, project administration, writing–review and editing.

Note: Supplementary data for this article are available at Cancer Immunology Research Online (http://cancerimmunolres.aacrjournals.org/).

incorporating null mutations of CD28 subdomains (YMNM, PRRP, or PYAP), we could optimize CAR T-cell costimulation and enhance function. *In vivo*, we found that mice given CAR T cells with only a PYAP CD28 endodomain had a significant survival advantage, with 100% of mice alive after 62 days compared with 50% for mice with an unmutated endodomain. We observed that mutant CAR T cells remained more sensitive to antigen after *ex vivo* antigen and PD-L1 stimulation, as demonstrated by increased cytokine production. The mutant CAR T cells also had a reduction of exhaustion-related transcription factors and genes such as *Nfatcl*, *Nr42a*, and *Pdcd1*. Our results demonstrated that CAR T cells with a mutant CD28 endodomain have better survival and function. This work allows for the development of enhanced CAR T-cell therapies by optimizing CAR T-cell costimulation.

Introduction

The therapeutic promise of T cells modified with chimeric antigen receptors (CAR) was realized when the FDA approved CD19-targeted CAR T cells for B-cell acute lymphoblastic leukemia (B-ALL) and aggressive B-cell lymphomas (1-3). However, there are limitations to approved CAR therapies, such as resistance and relapse. The design of the CAR, which includes an antigen-binding domain followed by the hinge, transmembrane, and signaling domains, has a significant impact on CAR T-cell function. One of the seminal observations that allowed the clinical evaluation of CAR T cells was the inclusion of a costimulatory domain with a CD3ζ activation domain that enhanced *in vivo* function compared with first-generation CARs that included only CD3ζ (4-6).

Although these early studies of CAR design evaluated qualitative outcomes, such as enhanced tumor killing, cytokine production, or *in vivo* persistence, more recent studies have focused on how CAR design regulates signaling and costimulation and the impact on function. One of the critical underlying mechanisms is that high tonic signaling, regardless of the costimulatory domain, induces T-cell exhaustion (7, 8). Conversely, in non-tonic signaling CARs, the type of costimulatory domain included can induce differential gene expression, T-cell subset formation, function, and exhaustion, with CD28-containing CARs driving more effector-like T cells prone to exhaustion and 4-1BB driving more memory-like T cells (9,10). These studies suggest that the type of costimulatory domain or quality of signaling regulates CAR T-cell function. Other studies show CD28 endodomains are associated with increased strength of CAR signaling and correlate with CAR T-cell exhaustion (11), and that reduced CAR activation, by the inclusion of a CD3ζ endodomain with null mutations at two ITAMs (immunoreceptor tyrosine-based activation motifs), supports T-cell differentiation toward memory and/or naïve subsets (12), suggesting that quantity of signaling affects CAR T-cell function.

These reports propose that a guiding principle for CAR design should be to reduce CAR signaling. However, we have previously demonstrated that increasing NF-κB in CAR T cells enhances proliferation, persistence, and *in vivo* function, in part by upregulating expression of antiapoptotic genes (13). These data highlight how signaling can result in an optimized function by induction of transcription factors that turn genes on and off. We hypothesized that exhaustion in CAR T cells with a CD28 endodomain is induced by specific signaling

pathways and transcription factors and not just the strength of signaling. CD28 includes at least three intracellular subdomains (YMNM, PRRP, and PYAP) that regulate costimulation post-T-cell receptor (TCR) stimulation, but it is unknown how each modulates CAR T-cell function. These three subdomains have important signaling capabilities. CD28 directly activates PI3K and Grb2 signaling through YMNM (14, 15), which drives terminal T-cell differentiation to short-lived effectors (16, 17). Previous work finds that mutation of YMNM to YMFM increases CAR T-cell persistence and antitumor durability in xenograft models (18). The PRRP motif can associate with ITK, which then signals through PLCγ and Erk, resulting in T-cell proliferation and IL2 production (19). The distal PYAP subdomain initiates signaling by binding LCK (20, 21), which has been confirmed in CARs (11, 22).

To evaluate our hypothesis, we created a series of CD28 endodomain mutations in a CD19-targeted CAR and evaluated their impact on *in vitro* function, *in vivo* function, and gene expression and accessibility. We determined that mutating the CD28 endodomain to preserve signaling through PYAP was sufficient for optimal *in vitro* and *in vivo* function. Our results also showed that mutated CD28 CAR T cells reduce the induction of NFAT and NR4A transcription factors, which has been associated with the upregulation of exhaustion-related genes in T cells (23, 24). Therefore, our work demonstrated that by attenuating transcription factors and genes associated with exhaustion, CAR T-cell function can be enhanced. These results provide insight into the design of CARs that enhance T-cell persistence and improve clinical responses.

Materials and Methods

Cells

All media and supplements were purchased from Thermo Fisher Scientific. Cell line sources, authentication, number of passages, and mycoplasma testing are provided in Supplementary Table S1. The Eμ-ALL cell line was previously generated and described (25). Eμ-ALL cells were cultured with irradiated (30 Gy) NIH/3T3 (ATCC) fibroblast feeder cells. The culture medium consisted of equal volumes of IMDM supplemented with 2 mmol/L L-glutamine, 55 μmol/L β-mercaptoethanol, penicillin (100 U/mL), streptomycin (100 μg/mL), and 10% FBS; and DMEM supplemented with 2 mmol/L L-glutamine, penicillin (100 U/mL), streptomycin (100 μg/mL),and 10% calf serum. To generate 3T3-mPD-L1 target cells, 1×10^5 NIH/3T3 cells (ATCC) were transduced with mouse PD-L1 (pLTC-mPD-L1; G&P Biosciences) using polybrene (8 μg/mL; Santa Cruz Biotechnology) for 24 hours according to the manufacturer's instructions. Cells expressing mPD-L1 were enriched for by puromycin antibiotic selection. 3T3-mCD19 target cells were previously generated and described (25). Mouse T-cell complete medium consisted of RPMI-1640 medium, 10% FBS, 2 mmol/L sodium pyruvate, 1 × nonessential amino acids, 10 mmol/L HEPES, 55 μmol/L β-mercaptoethanol, 2 mmol/L L-glutamine, penicillin (100 U/mL), and streptomycin (100 μg/mL). The NFAT luciferase reporter Jurkat stable cell line was purchased from Signosis and maintained and used according to the manufacturer's instructions. AP-1 luciferase reporter Jurkat stable cell line was produced by transducing Jurkat cells (ATCC) with Cignal Lenti AP1 Reporter-luc (Qiagen) particles according to the

manufacturer's instructions. Cells were tested for mycoplasma using the Universal Mycoplasma Detection Kit (ATCC).

Genetic constructs and CAR T-cell production

The SFG retroviral construct was used for all constructs, and m19Δz, m19z, m1928z, and m19hBBz CAR constructs have been described (13, 25). Mutated constructs replaced signaling subdomains in the CD28 costimulatory domain with amino acids as described (construct sequences in Supplementary Table S2; refs. 26, 27). Mut04 replaced PRRP and PYAP subdomains with ARRA and AYAA. Mut05 replaced YMNM and PYAP subdomains with FMNM and AYAA. Mut06 replaced YMNM and PRRP subdomains with FMNM and ARRA. All mouse CAR constructs had a glycine–serine linked mCherry reporter. In anti-human CD19 constructs, the SFG backbone was modified to include the FMC63 single-chain variable fragment (scFv) with CD8α transmembrane and hinge domain followed by CD28 or mut06 and CD3ζ.

All SFG constructs were transfected using a calcium phosphate transfection kit (Invitrogen) into 5×10^5 H29 cells [Sadelain Laboratory Memorial Sloan Kettering Cancer Center (MSKCC)] as previously described (28). Retroviral supernatants of transfected H29 were harvested and used to transduce Phoenix E or RD114 producer cells (Sadelain Laboratory MSKCC). Retroviral supernatant of producer cells was harvested, 0.45 μm filtered, and stored at −80°C until use. T cells were isolated from mouse splenocytes or whole PBMCs (AllCells) and transduced as described (13, 25, 28). Viability was measured by trypan blue staining and enumerated on an automated cell counter (Bio-Rad). Transduction efficiency was estimated by flow cytometry (as described below) as a percentage of $mCherry^+$ live cells or protein L^+ live cells for human CARs. For downstream experiments, CAR T-cell doses were normalized based on CAR gene transfer but not sorted to exclude CAR-negative T cells. As a result, the total T-cell dose was varied from 1.6×10^6 to 2.9×10^6.

Luciferase assays

2.5×10^6 of each Jurkat luciferase stable cell line was retrovirally transduced by 1-hour spin transduction with 1 mL of virus from the indicated CD19-targeted CAR constructs producer cells and incubated at 37°C for 24 hours. Live mCherry-positive cells were sorted with a FACSAria II cell sorter (BD Biosciences). 1×10^6 CAR-positive Jurkat luciferase cells were stimulated with 1×10^5 3T3-mCD19 target cells for 6 or 24 hours. After stimulation, cell lysates were prepared using Cell Culture Lysis Reagent (Promega). A luciferase assay was performed using the ONE-Glo luciferase assay system (Promega) according to the manufacturer's instructions. 20 μL of cell lysates per well were added to a 96-well white plate (Corning), followed by 100 μL of Luciferase Assay Reagent per well. Bioluminescence was measured on a SpectraMax L microplate luminometer (Molecular Devices). Each sample was measured in triplicate.

Western blot

A total of 9×10^6 CAR T cells per CAR were stimulated with 3T3-mCD19 target cells for 24 hours or left unstimulated. CAR T cells were sorted, as stated in the above section, and lysed with RIPA buffer. After protein quantification (Pierce Rapid Gold BCA Protein Assay

Kit; Thermo Scientific), 30 μg of lysate was loaded onto the gel. Proteins were detected using anti-pNFAT1 (1:1,000 milk; phospho S54; Abcam), anti-pLCK (1:500 milk; phospho Tyr394; Thermo Fisher), anti-NFAT1 (1:1,000 milk; Abcam), anti-LCK (1:1,000 milk; Invitrogen), and anti-S6 (1:400,000 milk; C.896.4; Thermo Fisher). Goat antirabbit IgG (H + L) and goat Anti-Mouse IgG (H + L; Jackson ImmunoResearch Laboratories, Inc.) were used as secondary antibodies. The secondary antibodies were diluted in milk at a concentration of 1:1,000, except for S6, which was at 1:5,000. Primary antibodies were incubated at 4°C for overnight, and secondary antibodies were incubated at room temperature for 2 hours. ChemiDocMP Imaging System (Bio-Rad) was used to detect ECL (Pierce ECL Western Blotting Substrate) Western blotting signals.

Mice

Animal studies were performed under protocols approved by the Institutional Animal Care and Use Committee of the University of South Florida. C57BL/6, Thy1.1 (B6.PL-*Thy1*^{a}/CyJ), Nur77^{GFP} (C57BL/6-Tg(Nr4a1-EGFP/cre)820Khog/J), and *Rag1*$^{-/-}$ (B6.129S7-*Rag1*^{tm1Mom}/J) mice were purchased from the Jackson Laboratory. Female and/or male mice at 8 to 12 weeks of age were used. NSG mice (NOD.Cg-*Prkdc*^{scid} *Il2rg*^{tm1Wjl}/SzJ) were purchased from the Jackson Laboratory and bred in our facility. For survival studies, mice were injected with Eμ-ALL (1×10^6 cells per mouse, day 0), followed by i.p. cyclophosphamide (300 mg/kg, day 6; Sigma-Aldrich) and CAR T cells (3×10^5 CAR T cells per mouse, day 7). Mice were monitored for illness daily and sacrificed when there was evidence of leukemia progression, such as decreased activity, hunched posture, or ruffled coat. At certain time points, blood was collected from the submandibular vein into tubes containing K3 EDTA (Sarstedt). At sacrifice, blood and/or femurs were collected. For blood samples, red blood cells were lysed using ACK buffer (Thermo Fisher) and stained for flow cytometry as described below. Bone marrow was isolated from femurs by cutting both ends of the femur and flushing it with a syringe containing PBS (Gibco). These cells were passed through a 70-μm cell strainer. Red blood cells were lysed as described above and stained for flow cytometry (described below). For *Rag1*$^{-/-}$ studies, mice were i.v. injected with 1×10^6 mCD19-targeted CAR T cells. Following 1 week after, *Rag1*$^{-/-}$ mice were i.v. injected with CAR T cells and were challenged with 1×10^6 Eμ-ALL cells. At sacrifice, spleens and femurs were collected. Femurs were processed as described above, and spleens crushed through a 70-μm cell strainer. For NSG studies, mice were i.v. injected with 5×10^5 Raji-GFP/luc cells at week –1, and 2×10^6 CAR T cells were i.v. injected at week 0. Tumors were measured using an IVIS Lumina III *In Vivo* Imaging System (PerkinElmer) for bioluminescence imaging (BLI) weekly for 3 weeks.

Flow cytometry

The following antibodies with clones listed were obtained from eBioscience: anti-mCD16/CD32 (clone 93), anti-mB220 (RA3-6B2), anti-mCD19 (eBio1D3), anti-mCD3 (145-2C11), anti-mCD4 (GK1.5), anti-mCD8 (53-6.7), anti-mPD1 (J43), anti-mLAG3 (eBioC9B7W), anti-mThy1.1 (HIS51), anti-mCD44 (1M7), anti-mCD62L (MEL-14), anti-mTER119 (TER-119), anti-mCD11b (M1/70), anti-mGr1 (RB6-8C5), anti-mNK1.1 (PK136), anti-mIFNγ (XMG1.2), and anti-TNFα (MP6-XT22). The following antibodies were from BioLegend: anti-mCD3 (17A2), anti-mCD4 (RM4-5), anti-mCD8 (clone 53-6.7), anti-mIL2

(JES6-5H4), and anti-hLAG3 (7H2C65). Anti-hTIM3 (7D3) and anti-hCD3 (SK7) were from BD Biosciences. Anti-hPD1 (eBioJ105), streptavidin Alexa Fluor 488 conjugate, Recombinant Protein L, biotinylated were purchased from Thermo Fisher Scientific.

T cells, blood, or bone marrow cells were first washed twice with PBS and stained with an ef450 fixable viability dye (eBioscience) at room temperature for 30 minutes. Surface staining was performed at 4°C with mouse BD Fc block (clone 2.4G2) and antibody mix in MACS buffer with 0.5% BSA (Miltenyi Biotec). For intracellular cytokine staining using the *Rag1*$^{-/-}$ mouse model, 1×10^6 splenocytes were cocultured with 1×10^5 irradiated 3T3-mCD19/mPDL1 target cells for 4 hours in the presence of 1 × protein transport inhibitor cocktail (eBioscience). Cells were then harvested, fixed, and permeabilized with Intracellular Fixation and Permeabilization Buffer Set (eBioscience) followed by antibody staining according to the manufacturer's instructions. For some experiments, Countbright beads (Thermo Fisher Scientific) were used for cell quantification. All samples were analyzed with a 5-laser LSRII (BD Biosciences), and data were analyzed using FlowJo software (Tree Star).

Cytokine immunoassay

CAR T cells (1×10^6) were cocultured with 1×10^5 3T3-mCD19 cells for 24 hours. Supernatants were collected, and 34 μL diluted 1:3 was analyzed using a Mouse Premixed Multi-Analyte Luminex Assay kit (R&D Systems) according to the manufacturer's instructions. Data were collected on a Luminex 100 system (Luminex), and concentrations were calculated using a five parameter logistic curve fit.

Cytotoxicity assay

Cytotoxicity assays were run on an xCelligence RTCA (real-time cell analysis) instrument (ACEA Biosciences) according to the manufacturer's instructions. Briefly, 1×10^4 3T3-mCD19 target cells were plated per well on an E-Plate 96. The next day, CAR T cells were resuspended in fresh complete medium without IL2 and added onto target cells at 10:1, 5:1, or 1:6 E:T ratios, and growth was monitored up to 172 hours.

RNA sequencing and ATAC-seq

All samples were prepared in biological duplicates. CAR T cells were stimulated with 3T3-mCD19 target cells at a 10:1 E:T ratio for 24 hours. Cells were sorted using a FACSAria II cell sorter (BD Biosciences) gating on live CAR$^+$ cells. Samples were then pelleted and snap-frozen in liquid nitrogen. Total RNA was isolated from the cells using the Qiagen RNeasy Mini Kit (Qiagen, cat.#74104).RNA Integrity Number (RIN) was determined for each sample using TapeStation 4150 System (Agilent). Samples with RIN values above 7.0 were used for downstream library prep. For each sample, 2 μg of total RNA was then used in Illumina's TruSeq Stranded mRNA Library kit (cat. #20020594). Libraries were sequenced on Illumina NextSeq 500 as paired-end 75-nt reads. RNA sequencing (RNA-seq) was performed by Active Motif (Carlsbad, CA) using 100-nt sequence reads by an Illumina HiSeq 4000. The reads were then mapped to the genome using the STAR algorithm (v2.5.2b; https://github.com/alexdobin/STAR/blob/master/doc/STARmanual.pdf) with the default setting. For ATAC-seq, Active Motif performed paired-end 42-bp sequencing reads

generated by Illumina sequencing (NextSeq 500) and were mapped to the genome using the BWA algorithm (https://github.com/lh3/bwa/releases/tag/0.7.12; ref. 29) with default settings. Only reads that passed Illumina's purity filter, aligned with no more than two mismatches, and mapped uniquely to the genome were used in the subsequent analysis. Duplicate reads were removed. RNA-seq and ATAC-seq data are deposited in the NCBI's Gene Expression Omnibus database under GEO accession number GSE142506.

Statistical analysis

Means were compared using a nonparametric one-way ANOVA and then using a *t* test to compare multiple means. Survival was compared using a log-rank test. Statistical analyses were conducted using GraphPad Prism software 7. $P \leq 0.05$ was considered statistically significant.

Results

m1928z CAR T cells are less sensitive to antigen compared with m19hBBz

To evaluate mechanisms regulating CAR T-cell persistence *in vivo*, we used four mouse CD19-targeted (mCD19-targeted) CARs in *Rag1*$^{-/-}$ mice. We used *Rag1*$^{-/-}$ mice to examine CAR T-cell persistence in a setting where we could control exposure to antigen. All CARs have been described (13) and are murine derived with the same rat-origin anti-mCD19 scFv paired to a mouse CD8α hinge and transmembrane domain. They differ in their intracellular activation and costimulatory domains by having either a nonfunctional CD3ζ domain (m19dz), CD3ζ alone (m19z), or CD3ζ paired with a CD28 (m1928z) or 4-1BB costimulatory domain (m19hBBz). We i.v. injected 1×10^6 CAR T cells into each *Rag1*$^{-/-}$ mouse. For the early time point, mice received CAR T cells at week 0, CD19-positive antigen (Eμ-ALL cells) at week 1, and sacrificed at week 2. For the late time point, separate mice were given CAR T cells at week 0, Eμ-ALL cells at week 5, and sacrificed at week 6. Control mice received T cells, but no Eμ-ALL cells. Upon sacrifice, total donor and CAR T cells were enumerated. CAR T-cell numbers increased from week 1 to 2 and then stabilized from weeks 2 to 6 (Fig. 1A). Without any antigen stimulation, T cells modified with a CAR containing a 4-1BB endodomain expanded the most, which is consistent with prior studies (30). At the early time point, all groups except m19dz appeared sensitive to antigen with the highest number of donor T cells in the m19hBBz group (5.5×10^4), followed by m1928z (3.3×10^4), m19z (1.5×10^4), and m19dz (1.3×10^4) groups (Fig. 1B). However, at the later time point, we only detected significant antigen-dependent cell expansion in the m19hBBz CAR T-cell group (Fig. 1C-D). This observation led us to examine the immune phenotypes of m1928z and m19hBBz CAR T cells after antigen stimulation. m1928z CAR T cells had an increase in the central memory (CM) T cells (Fig. 1E), but they also had higher expression of exhaustion markers PD-1 (Fig. 1F) and LAG3 (Fig. 1G). Although PD-1 can also be an activation marker, the coincident expression of LAG3 in these cells suggested that increased exhaustion resulted in m1928z CAR T cells' decreased sensitivity to antigen. Previous studies (7, 9, 10) have demonstrated that quantity or quality of signaling can contribute to exhaustion, so we reasoned that targeted mutations of the CD28 endodomain could attenuate CAR T-cell exhaustion.

CD28-mutant CAR T-cell *in vitro* characterization

We mutated the CD28 costimulatory subdomains to create CARs that retained only one functional CD28 motif (Fig. 2A). We confirmed these mutations did not alter CAR gene transfer (Fig. 2B) or mean fluorescence intensity (MFI; Fig. 2C). CAR T-cell viability (Fig. 2D) and proliferation (Fig. 2E) before antigen exposure were also unchanged. We examined CAR T-cell cytokine production after a 24-hour stimulation with 3T3-mCD19 cells and determined that mutants 04, 05, and 06 had a significant reduction in IFNγ (Fig. 3A), IL6 (Fig. 3B), IL2 (Fig. 3C), and TNFα (Fig. 3D) compared with m1928z CAR T cells. However, IFNγ, IL6, and TNFα were still significantly higher than m19z CAR T cells. We also evaluated CAR T-cell cytotoxicity using a real-time killing assay and determined that at a high (10:1) effector-to-target (E:T) ratio, mutated CAR T cells killed similarly to those with m1928z (Fig. 3E). With a low (1:6) E:T ratio, we found a significant enhancement in mut06 cytotoxicity compared with the other mutants or cells with m1928z at 48 hours (Fig. 3F). These results demonstrated that T cells modified with a CAR containing a mutated CD28 costimulatory domain could still enhance cytokine production and killed at similar or better levels compared with m1928z CAR T cells.

We also examined the function of $CD4^+$ and $CD8^+$ CAR T cells separately to determine if mut06 was affecting their functions. $CD4^+$ or $CD8^+$ T cells from splenocytes were isolated and then transduced with the CAR (Supplementary Fig. S1A). We found that mut06 $CD4^+$ and $CD8^+$ T cells were less cytotoxic compared with those with m1928z (Supplementary Fig. S1B). We also found that $CD8^+$ CAR T cells for both mut06 and m1928z cells secreted more IFNγ and TNFα compared with $CD4^+$ cells, whereas IL6 was secreted in similar amounts by both $CD4^+$ and $CD8^+$ CAR T cells (Supplementary Fig. S1C). These results suggested that mut06 required both $CD4^+$ and $CD8^+$ T cells for optimal function.

Mut06 CAR T cells support enhanced *in vivo* function

We next compared the *in vivo* function of mut04–06 CAR T cells using immune-competent mice (13). To examine CAR T-cell persistence and B-cell killing, we i.v. injected 3×10^5 CAR T cells 1 day after conditioning C57BL/6 mice with 300 mg/kg of intraperitoneal (i.p.) cyclophosphamide. All CAR T cells injected into mice exhibited a similar phenotype (Supplementary Fig. S2). We collected blood at 1, 2, 4, and 6 weeks to monitor CAR T-cell persistence and B-cell aplasia. At 4 weeks, mice given mut06 CAR T cells had significantly fewer B cells on average (48 per μL of blood) compared with mice given m19z (1,874 per μL), mut04 (1,857 per μL), or mut05 (1,509 per μL) and showed similar B-cell aplasia compared with mice given m1928z (315 per μL) CAR T cells (Fig. 4A). We also found that mut06 CAR T cells had the highest number of CAR T cells in the blood (77.6 per μL) 1 week after injection. After 8 weeks, we found that mice in the m1928z and mut06 CAR groups were the only ones to have persisting CAR T cells in the bone marrow. Mice given m1928z CAR T cells or mut06 CAR T cells had a significantly lower percentage of B cells compared with mice given m19z CAR T cells (Fig. 4B). We also found no significant differences in the number of effector memory (EM) or CM CAR T cells (Fig. 4C). These results identified mut06 as the superior CAR compared with mut04 and mut05. Therefore, we focused the remainder of our studies on mut06.

To compare the *in vivo* function of mut06 CAR T cells using a B-ALL mouse model (13, 25), C57BL/6 mice were i.v. injected with 1×10^6 Eμ-ALL cells, 1 week later treated with 300 mg/kg i.p. cyclophosphamide, and 1 day later with 3×10^5 CAR T cells (Supplementary Fig. S3). At this stress-test dose, mice given mut06 CAR T cells had a 100% survival rate out to 62 days, whereas mice with m1928z CAR T cells had a 50% survival rate consistent with our prior published studies (Fig. 4D; refs. 13, 25). These data demonstrated that the preservation of PYAP, while eliminating YMNM and PRRP subdomains, was not deleterious and supported efficacious *in vitro* and *in vivo* function.

To validate the efficacy of mut06 using a different scFv and human T cells, we generated fully humanized versions of CD28, 4-1BB, and mut06 CARs. Each CAR used the human FMC63 anti-CD19 scFv. Consistent with our mouse data, we found that human (h)mut06 had no appreciable effect on cell viability or proliferation (Supplementary Fig. S4A). We determined that at a 5:1 E:T ratio, hmut06 CAR T cells killed similarly to h1928z CAR T cells (Supplementary Fig. S4B). We also stimulated CAR T cells with 3T3-hCD19 cells and, after 14 days, examined LAG3, TIM3, and PD-1 expression. Hmut06 CAR T cells had significantly decreased expression of LAG3 and TIM3 compared with those with h1928z (Supplementary Fig. S4C). We also found that hmut06 CAR T cells were better able to control lymphoma growth in NSG mice compared with CAR T cells with h1928z (Supplementary Fig. S5A-S5B).

Mut06 CAR T cells are more sensitive to antigen compared with m1928z CAR T cells

We examined what effect the CD28 costimulatory domain mutations had on the CAR's antigen-dependent responses. *Rag1*$^{-/-}$ mice were i.v. injected with 1×10^6 Eμ-ALL cells 1 week after i.v. injection of 1×10^6 CART cells (Supplementary Fig. S6). The following week, mice were sacrificed, and we found a similar percentage of CAR$^+$ cells in the m1928z and mut06 groups (Fig. 5A; Supplementary Fig. S7A). We detected a significant increase in CAR$^+$CD8$^+$ T cells in the mut06 CAR group compared with the m1928z group (Fig. 5A; Supplementary Fig. S7B). There was no significant difference in CM (17.7% vs. 23.2) and EM (2.1% vs. 1.7%) cells between m1928z and mut06 groups (Fig. 5A; Supplementary Fig. S7C). PD-1 expression was similar for both m1928z and mut06 groups (Fig. 5A; Supplementary Fig. S7D). The similarity in PD-1 expression was possibly due to the 2-week post CAR T-cell injection time point. To determine functional exhaustion and if mut06 CAR T cells remained sensitive to antigen, we isolated and *ex vivo*–stimulated splenocytes from *Rag1*$^{-/-}$ mice with 3T3 cells expressing mCD19 and mPD-L1 for 4 hours and examined cytokine production. Our results demonstrated that mut06 CAR T cells produced significantly more TNFα (Fig. 5B; Supplementary Fig. S7E) and IL2 (Fig. 5B; Supplementary Fig. S7F), and compared with m1928z CAR T cells after antigen stimulation and PD-1 ligation. Higher secretion of cytokines by mut06 suggested they were less functionally exhausted compared with m1928z cells.

Mut06 CAR T cells have a reduction in exhaustion-related transcription factors

Previous work has found that CD28 subdomains bind PI3K, GRB2, ITK, and LCK, which mediate downstream signaling, leading to T-cell activation and/or exhaustion (Fig. 6A). To determine if increased function was related to signaling and/or transcription factors, we

examined Nur77 expression in CAR T cells with different costimulatory domains. *Nur77*^{GFP} mice were used as the source of T cells for transduction. These mice have a GFP-Cre fusion protein inserted at the start codon of *Nr4a1* (Nur77), which is activated by antigen binding in lymphocytes (31). These mice were previously used to demonstrate that Nur77 expression correlated with TCR signaling strength, and we postulated that it might also correlate with CAR signaling strength. Nur77 transcription factors are associated with T-cell exhaustion (32). Evaluation of Nur77 after CAR stimulation found that mut06 CAR T cells had significantly lower Nur77 expression (MFI = 352) than m1928z CAR T cells (MFI = 490; Fig. 6B). Also, we examined transcription factors in Jurkat luciferase reporters and found that mut06 Jurkat cells had significantly reduced expression of NFAT and AP1 (Fig. 6C-D). Phospho-NFAT by Western blot was decreased in mut06 CAR T cells compared with m1928z cells (Fig. 6E; Supplementary Fig. S8B). We also found that after 24-hour antigen stimulation, GRB2 did not physically interact with m19dz, m1928z, or mut06 (Supplementary Fig. S8C). Considering that all of these transcription factor pathways give input for T-cell exhaustion, it suggested that optimized CD28 costimulation limited the induction of transcription factors associated with exhaustion.

Mut06 has reduced exhaustion-related gene expression and accessibility

Our data demonstrated that mut06 attenuated exhaustion-related transcription factors. We found that 24 hours after antigen encounter, exhaustion-related transcription factors, such as Nur77, were enhanced in m1928z compared with m19hBBz and mut06 CAR T cells (Supplementary Fig. S9). With these data, we wanted to examine exhaustion-related transcription factor gene expression after a 24-hour antigen stimulation. We chose 24 hours for comparisons because we reasoned that this would allow more fine-tuning in CAR design if we could identify transcription factors and/or gene expression features at this early time point that could lead to exhaustion over time. We confirmed that transcription factors associated with exhaustion could already be detected at increased levels in m1928z compared with mut06 CAR T cells (Fig. 6). Studies have identified a subset of genes that are important for T-cell exhaustion (23, 33). Wherry and colleagues (33) reports 78 genes upregulated in exhausted T cells. When we examined these genes in our CAR T cells by RNA-seq, we found they were more upregulated in m1928z compared with mut06 or m19hBBz CAR T cells (Fig. 7A). We next looked at 22 genes upregulated when NFAT was constitutively active, which also overlaps with the identified gene set (23, 33). Many of these exhaustion-related genes were upregulated in m1928z CAR T cells, whereas they were decreased in m19hBBz cells (Fig. 7B). The mut06 CAR T-cell gene-expression pattern was more similar to m19hBBz CAR T cells, with exhaustion-related genes downregulated compared with those with m1928z.

Previous work has shown that NFAT controls T-cell exhaustion by binding directly to the regulatory regions of exhaustion-associated genes (23, 33). To compare differences in the accessibility of exhaustion-related genes, we performed ATAC-seq. Consistent with the luciferase reporter data (Fig. 6C-D), NFAT (*Nfatcl*) and AP1 components Jun (*Jun*) and Fos (*Fos*) had lower chromatin accessibility profiles in mut06 CAR T cells compared with those with m1928z (Fig. 7C). We also saw that Nur77 (*Nr4a1*) had less accessibility in mut06 and m19hBBz CAR T cells compared with m1928z cells, supporting our previous observations.

We also found that exhaustion-related genes *Havcr2* (TIM3), *Pdcd1* (PD-1), and *Lag3* (LAG3) all had reduced chromatin accessibility in mut06 CAR T cells compared with m1928z cells. TNFα (*Tnf*), a vital effector cytokine for CAR T cells, had chromatin accessibility that was similar in all three groups. Although the *Pdcd1* locus was more accessible in m1928z CAR T cells than mut06 CAR T cells, the protein expression of PD-1 was similar (Fig. 5). We speculate this was likely due to the different time points measured after antigen stimulation in ATAC-seq (24 hours) versus *in vivo* antigen challenge (Fig. 5; 1 week). These genomic studies support our findings that mut06 CAR T-cell costimulation lowers transcription factors that support less expression of exhaustion-related genes, which contributes to its support of enhanced T-cell function.

Discussion

Previous research has evaluated how CAR design affects signaling and function. The type of costimulatory domain in a CAR induces different T-cell gene expression, phenotype, effector function, and exhaustion (7, 9, 10). These studies suggest that the quantity of costimulation affects CAR T-cell function. The CD28 endodomain has been reported to have increased strength of CAR signaling, correlating with CAR T-cell exhaustion (11). We showed that m1928z CAR T cells were less sensitive to antigen compared with m19hBBz CAR T cells *in vivo*. We believe this was due to exhaustion within the CM subsets, which was reflected by their increased expression of PD-1 and LAG3. Although increased CM CAR T cells in the m1928z group is inconsistent with prior studies (9, 10), this may be due to the different models used, with one involving alloreactive CAR T cells in a model of stem cell transplantation and the other relying on immune phenotyping of human CM CAR T cell subsets. However, we have shown that the 4-1BB endodomain in our mouse CARs enhanced function associated with memory, such as persistence, proliferation, and antiapoptosis protein upregulation compared with the CD28 endodomain (13). We attributed this functional enhancement to the upregulation of NF-κB, which was also confirmed by a group comparing CD28 and 4-1BB endodomains in human CARs (34). Therefore, we believe, based on functional analyses, that our CARs were consistent with the enhancement of memory by 4-1BB compared with CD28.

Previous work shows that null mutations in CD3ζ ITAM domains reduce CAR T-cell activation resulting in a more memory/naïive phenotype (12). This observation suggests that any reduction in CAR signaling will be beneficial. However, we and others have demonstrated that increasing the NF-κB transcription factor in CAR T cells enhances proliferation, persistence, and *in vivo* function (13, 34). Work using mutations in CD28 and ICOS costimulatory domains finds that mutating YMNM to YMFM promotes durable antitumor control in xenograft models (18). This study is further evidence that the quality of costimulation can affect CAR T-cell function, not just quantity. Therefore, we hypothesized that transcription factors, controlled by the quality or type of signaling and not just quantity, regulate the exhaustion of CAR T cells.

To evaluate CD28 costimulation, we designed a series of null mutations in the YMNM, PRRP, or PYAP subdomains. These CARs included two mutated subdomains, leaving only a single functional subdomain. Our CAR T cells with mutated CD28 costimulatory domains

still produced cytokines and killed at similar levels to second-generation CAR T cells, showing that just reducing signaling does not result in an inadequate response. A limitation to studies evaluating CAR T cells is a reliance on *in vitro* assays or NSG mice, which are unable to model cellular immunobiology such as exhaustion. Therefore, we evaluated CD19-targeted CAR T cells in an immunocompetent Eμ-ALL animal model. Eliminating signaling from the YMNM and PRRP CD28 subdomains (mut06) enhanced CAR T-cell persistence and survival *in vivo*. The mut06 CAR T cells had increased sensitivity to antigen compared with m1928z CAR T cells *in vivo*. We demonstrated that mut06 CAR T cells secreted more cytokines than m1928z CAR T cells when stimulated with both the CD19 antigen and PD-L1, despite these CAR T cells expressing similar PD-1. Considering that one known mechanism for PD-1–induced exhaustion in T cells is by dephosphorylation of CD28 (35), we speculate that the mut06 endodomain may be less sensitive to dephosphorylation, which is a mechanism we are evaluating.

In contrast, we found that mut04 and mut05 did not enhance CAR function, even though these mutants had reduced CD28 signaling. These data support previous work, which shows the quality of costimulatory signaling based on the positioning of the signaling domains, not the overall quantity of signaling, results in enhanced CAR T-cell persistence and efficacy (36). Another study also finds that balancing activation signals through optimizing CD28 costimulation results in CAR T cells with a more effective antitumor function (37). Together, these results suggest a model of CAR costimulation in which some signaling pathways are critical and others expendable for enhanced function.

To evaluate how optimized CAR costimulation enhanced CAR T-cell function, we examined NFAT/AP1/Nur77-dependent exhaustion (17). The transcription factor Nur77 (*Nr4a1*) was higher in m1928z compared with mut06 CAR T cells. NFAT has also been shown to directly induce exhaustion-related genes in $CD8^+$ T cells (23). Our results showed that mut06 had reduced NFAT (*Nfatc1*) transcription and phosphorylation compared with m1928z CAR T cells. ATAC-seq demonstrated that *Nfatc1* was less accessible in mut06 CAR T cells. We also found that *Nr4a1* and *Nr4a2* were less accessible compared with m1928z, which is consistent with reports showing CAR T cells lacking NR4A transcription factors promote tumor regression and prolong survival (32). We examined the expression of 22 exhaustion-related genes by RNA-seq and found that mut06 had less expression of those genes compared with m1928z CAR T cells.

We found that CAR signaling quality plays a vital role in CAR T-cell function and persistence. We showed that PYAP-dependent signaling alone could enhance CD28-based CAR T-cell function. This finding suggests LCK is a crucial pathway for CAR T-cell function and that only reducing CAR signaling may not improve outcomes. Other groups have also investigated LCK signaling in CAR T cells and show that deleting the PYAP binding domain in CD28 CAR T cells increases antitumor responses by reducing IL2 (38, 39). We believe there are two possibilities for why CARs with different mutations, one that preserves and the other that deletes the PYAP motif, can both enhance T-cell function. The quantity of signaling may be the critical regulator for CAR T-cell exhaustion so that anything that reduces CD28 costimulation enhances CAR T-cell function, which is supported by studies involving strength and/or tonicity of CAR signaling and activation

(7-9). However, this might also be due to different experimental systems with a similar qualitative focus, enhancement of CAR T-cell function, but different mechanistic evaluations. We are not certain how PYAP mutations affect exhaustion-related transcription factors and gene accessibility nor if preservation of the PYAP subdomain alone, as in the mut06 CAR, reduces regulatory T-cell (Treg) formation, which was reported by the Abken group to be a mechanism for enhanced CAR T-cell function (39, 40). However, we did observe the mut06 CAR reduced IL2 secretion, which is reported (39) to be the mediator for reducing Treg maintenance. Another study has shown, using a proteomics approach, that CARs with CD28 costimulatory domains have superior therapeutic efficacy because of enhanced LCK recruitment (41). Similarly, LCK-mediated signaling is critical for CAR T cells with a CD8α transmembrane domain (11), and recruitment of LCK to the CAR synapse can enhance tumor killing in 4-1BB CARs (22). Ultimately, these mutations will be best evaluated in patients to determine how they affect clinical outcomes.

Our work demonstrated that the PYAP subdomain, which binds LCK, was critical for optimized CD28 costimulation in CAR T cells. Our results also demonstrated that the function of second-generation CAR T cells could be optimized by modulating the CD28 costimulatory domain and suggests the potential for clinical translation by using drugs that target the signaling pathways of NFAT and/or NR4A.

Supplementary Material

Refer to Web version on PubMed Central for supplementary material.

Acknowledgments

The authors thank the Abate-Daga lab for help with the xCelligence killing assay. This work has been supported in part by the Flow Cytometry Core Facility at Moffitt Cancer Center, an NCI-designated Comprehensive Cancer Center (P30-CA076292). This work has been supported in part by the Biostatistics and Bioinformatics Core at the H. Lee Moffitt Cancer Center and Research Institute, a Comprehensive Cancer Center designated by the NCI and funded in part by Moffitt's Cancer Center Support Grant (P30-CA076292). This work was supported by funds from the H. Lee Moffitt Cancer Center and Research Institute to M.L. Davila. This study was supported in part by research funding from Atara Biotherapeutics to M.L. Davila.

The costs of publication of this article were defrayed in part by the payment of page charges. This article must therefore be hereby marked *advertisement* in accordance with 18 U.S.C. Section 1734 solely to indicate this fact.

References

1. Neelapu SS, Locke FL, Bartlett NL, Lekakis LJ, Miklos DB, Jacobson CA, et al. Axicabtagene ciloleucel CAR T-cell therapy in refractory large B-cell lymphoma. N Engl J Med 2017;377:2531–44. [PubMed: 29226797]
2. Maude SL, Laetsch TW, Buechner J, Rives S, Boyer M, Bittencourt H, et al. Tisagenlecleucel in children and young adults with B-cell lymphoblastic leukemia. N Engl J Med 2018;378:439–48. [PubMed: 29385370]
3. Schuster SJ, Bishop MR, Tam CS, Waller EK, Borchmann P, McGuirk JP, et al. Tisagenlecleucel in adult relapsed or refractory diffuse large B-cell lymphoma. N Engl J Med 2019;380:45–56. [PubMed: 30501490]
4. Brentjens RJ, Latouche JB, Santos E, Marti F, Gong MC, Lyddane C, et al. Eradication of systemic B-cell tumors by genetically targeted human T lymphocytes co-stimulated by CD80 and interleukin-15. Nat Med 2003;9:279–86. [PubMed: 12579196]

5. Imai C, Mihara K, Andreansky M, Nicholson IC, Pui CH, Geiger TL, et al. Chimeric receptors with 4-1BB signaling capacity provoke potent cytotoxicity against acute lymphoblastic leukemia. Leukemia 2004;18:676–84. [PubMed: 14961035]
6. Kowolik CM, Topp MS, Gonzalez S, Pfeiffer T, Olivares S, Gonzalez N, et al. CD28 costimulation provided through a CD19-specific chimeric antigen receptor enhances in vivo persistence and antitumor efficacy of adoptively transferred T cells. Cancer Res 2006;66:10995–1004. [PubMed: 17108138]
7. Long AH, Haso WM, Shern JF, Wanhainen KM, Murgai M, Ingaramo M, et al. 4-1BB costimulation ameliorates T cell exhaustion induced by tonic signaling of chimeric antigen receptors. Nat Med 2015;21:581–90. [PubMed: 25939063]
8. Gomes-Silva D, Mukherjee M, Srinivasan M, Krenciute G, Dakhova O, Zheng Y, et al. Tonic 4-1BB costimulation in chimeric antigen receptors impedes T cell survival and is vector-dependent. Cell Rep 2017;21:17–26. [PubMed: 28978471]
9. Zhao Z, Condomines M, van der Stegen SJ, Perna F, Kloss CC, Gunset G, et al. Structural design of engineered costimulation determines tumor rejection kinetics and persistence of CAR T cells. Cancer Cell 2015;28:415–28. [PubMed: 26461090]
10. Ghosh A, Smith M, James SE, Davila ML, Velardi E, Argyropoulos KV, et al. Donor CD19 CAR T cells exert potent graft-versus-lymphoma activity with diminished graft-versus-host activity. Nat Med 2017;23:242–9. [PubMed: 28067900]
11. Salter AI, Ivey RG, Kennedy JJ, Voillet V, Rajan A, Alderman EJ, et al. Phosphoproteomic analysis of chimeric antigen receptor signaling reveals kinetic and quantitative differences that affect cell function. Sci Signal 2018;11:eaat6753. [PubMed: 30131370]
12. Feucht J, Sun J, Eyquem J, Ho YJ, Zhao Z, Leibold J, et al. Calibration of CAR activation potential directs alternative T cell fates and therapeutic potency. Nat Med 2019;25:82–8. [PubMed: 30559421]
13. Li G, Boucher JC, Kotani H, Park K, Zhang Y, Shrestha B, et al. 4-1BB enhancement of CAR T function requires NF-kappaB and TRAFs. JCI Insight 2018;3:e121322.
14. Truitt KE, Hicks CM, Imboden JB. Stimulation of CD28 triggers an association between CD28 and phosphatidylinositol 3-kinase in Jurkat T cells. J Exp Med 1994;179:1071–6. [PubMed: 7509360]
15. Parry RV, Reif K, Smith G, Sansom DM, Hemmings BA, Ward SG. Ligation of the T cell co-stimulatory receptor CD28 activates the serine-threonine protein kinase protein kinase B. Eur J Immunol 1997;27:2495–501. [PubMed: 9368602]
16. Macintyre AN, Finlay D, Preston G, Sinclair LV, Waugh CM, Tamas P, et al. Protein kinase B controls transcriptional programs that direct cytotoxic T cell fate but is dispensable for T cell metabolism. Immunity 2011;34:224–36. [PubMed: 21295499]
17. Boomer JS, Green JM. An enigmatic tail of CD28 signaling. Cold Spring Harb Perspect Biol 2010;2:a002436. [PubMed: 20534709]
18. Guedan S, Madar A, Casado-Medrano V, Shaw CE, Wing A, Liu F, et al. Single residue in CD28-costimulated CAR T cells limits long-term persistence and antitumor durability. J Clin Invest 2020;130:3087–97. [PubMed: 32069268]
19. Gomez-Rodriguez J, Kraus ZJ, Schwartzberg PL. Tec family kinases Itk and Rlk / Txk in T lymphocytes: cross-regulation of cytokine production and T-cell fates. FEBS J 2011;278:1980–9. [PubMed: 21362139]
20. King PD, Sadra A, Teng JM, Xiao-Rong L, Han A, Selvakumar A, et al. Analysis of CD28 cytoplasmic tail tyrosine residues as regulators and substrates for the protein tyrosine kinases, EMT and LCK. J Immunol 1997;158:580–90. [PubMed: 8992971]
21. Holdorf AD, Green JM, Levin SD, Denny MF, Straus DB, Link V, et al. Proline residues in CD28 and the Src homology (SH)3 domain ofLck are required for T cell costimulation. J Exp Med 1999;190:375–84. [PubMed: 10430626]
22. Sun C, Shou P, Du H, Hirabayashi K, Chen Y, Herring LE, et al. THEMIS-SHP1 recruitment by 4-1BB tunes LCK-mediated priming of chimeric antigen receptor-redirected T cells. Cancer Cell 2020;37:216–25. [PubMed: 32004441]

23. Martinez GJ, Pereira RM, Aijo T, Kim EY, Marangoni F, Pipkin ME, et al. The transcription factor NFAT promotes exhaustion of activated CD8(+) T cells. Immunity 2015;42:265–78. [PubMed: 25680272]
24. Philip M, Fairchild L, Sun L, Horste EL, Camara S, Shakiba M, et al. Chromatin states define tumour-specific T cell dysfunction and reprogramming. Nature 2017;545:452–6. [PubMed: 28514453]
25. Davila ML, Kloss CC, Gunset G, Sadelain M. CD19 CAR-targeted T cells induce long-term remission and B cell aplasia in an immunocompetent mouse model of B cell acute lymphoblastic leukemia. PLoS One 2013;8:e61338. [PubMed: 23585892]
26. Friend LD, Shah DD, Deppong C, Lin J, Bricker TL, Juehne TI, et al. A dose-dependent requirement for the proline motif of CD28 in cellular and humoral immunity revealed by a targeted knockin mutant. J Exp Med 2006;203:2121–33. [PubMed: 16908623]
27. Dodson LF, Boomer JS, Deppong CM, Shah DD, Sim J, Bricker TL, et al. Targeted knock-in mice expressing mutations of CD28 reveal an essential pathway for costimulation. Mol Cell Biol 2009;29:3710–21. [PubMed: 19398586]
28. Li G, Park K, Davila ML. Gammaretroviral production and T cell transduction to genetically retarget primary T cells against cancer. Methods Mol Biol 2017;1514:111–8. [PubMed: 27787796]
29. Li H, Durbin R. Fast and accurate short read alignment with Burrows-Wheeler transform. Bioinformatics 2009;25:1754–60. [PubMed: 19451168]
30. Milone MC, Fish JD, Carpenito C, Carroll RG, Binder GK, Teachey D, et al. Chimeric receptors containing CD137 signal transduction domains mediate enhanced survival of T cells and increased antileukemic efficacy in vivo. Mol Ther 2009;17:1453–64. [PubMed: 19384291]
31. Moran AE, Holzapfel KL, Xing Y, Cunningham NR, Maltzman JS, Punt J, et al. T cell receptor signal strength in Treg and iNKT cell development demonstrated by a novel fluorescent reporter mouse. J Exp Med 2011;208:1279–89. [PubMed: 21606508]
32. Chen J, Lopez-Moyado IF, Seo H, Lio CJ, Hempleman LJ, Sekiya T, et al. NR4A transcription factors limit CAR T cell function in solid tumours. Nature 2019;567:530–4. [PubMed: 30814732]
33. Wherry EJ, Ha SJ, Kaech SM, Haining WN, Sarkar S, Kalia V, et al. Molecular signature of CD8+ T cell exhaustion during chronic viral infection. Immunity 2007;27:670–84. [PubMed: 17950003]
34. Philipson BI, O'Connor RS, May MJ, June CH, Albelda SM, Milone MC. 4-1BB costimulation promotes CAR T cell survival through noncanonical NF-kappaB signaling. Sci Signal 2020;13:eaay8248. [PubMed: 32234960]
35. Hui E, Cheung J, Zhu J, Su X, Taylor MJ, Wallweber HA, et al. T cell costimulatory receptor CD28 is a primary target for PD-1-mediated inhibition. Science 2017;355:1428–33. [PubMed: 28280247]
36. Guedan S, Posey AD Jr, Shaw C, Wing A, Da T, Patel PR, et al. Enhancing CAR T cell persistence through ICOS and 4-1BB costimulation. JCI insight 2018;3:e96976.
37. Wijewarnasuriya D, Bebernitz C, Lopez AV, Rafiq S, Brentjens RJ. Excessive costimulation leads to dysfunction of adoptively transferred T cells. Cancer Immunol Res 2020;8:732–42. [PubMed: 32213625]
38. Gulati P, Ruhl J, Kannan A, Pircher M, Schuberth P, Nytko KJ, et al. Aberrant Lck signal via CD28 costimulation augments antigen-specific functionality and tumor control by redirected T cells with PD-1 blockade in humanized mice. Clin Cancer Res 2018;24:3981–93. [PubMed: 29748183]
39. Kofler DM, Chmielewski M, Rappl G, Hombach A, Riet T, Schmidt A, et al. CD28 costimulation Impairs the efficacy of a redirected t-cell antitumor attack in the presence of regulatory T cells which can be overcome by preventing Lck activation. Mol Ther 2011;19:760–7. [PubMed: 21326215]
40. Hombach AA, Abken H. Costimulation by chimeric antigen receptors revisited the T cell antitumor response benefits from combined CD28-OX40 signalling. Int J Cancer 2011;129:2935–44. [PubMed: 22030616]
41. Ramello MC, Benzaid I, Kuenzi BM, Lienlaf-Moreno M, Kandell WM, Santiago DN, et al. An immunoproteomic approach to characterize the CAR interactome and signalosome. Sci Signal 2019;12:eaap9777. [PubMed: 30755478]

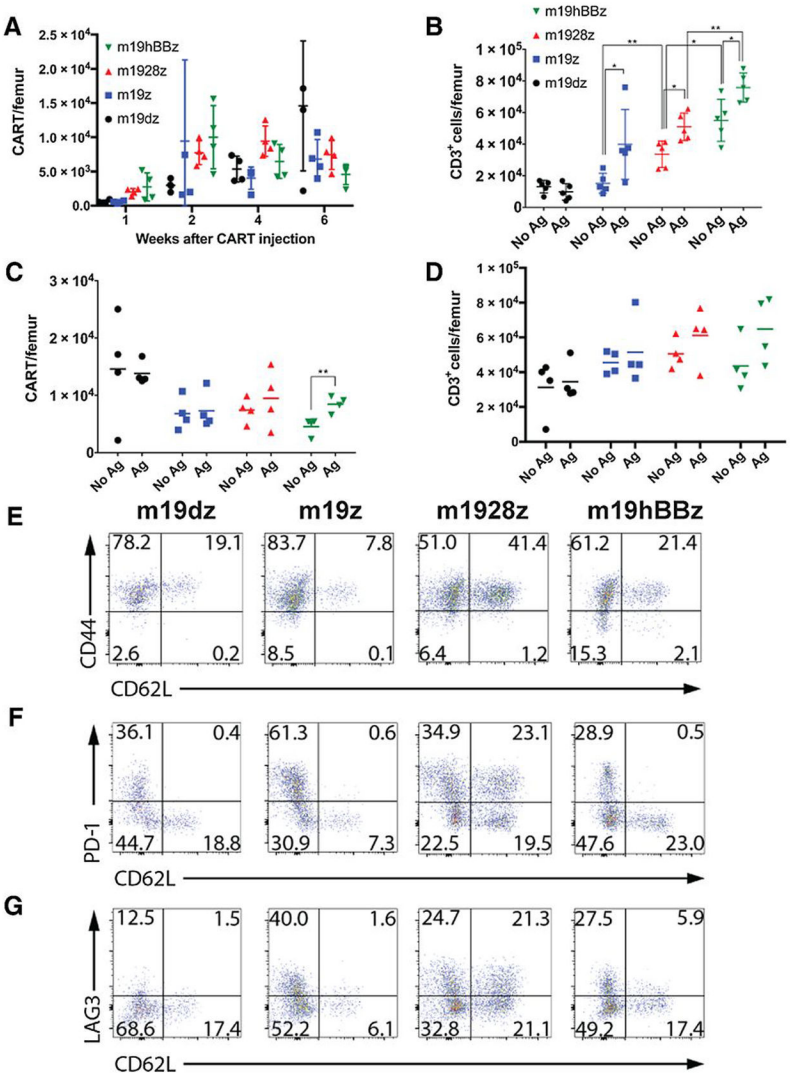

Figure 1.

m1928z CAR T cells are less sensitive to antigen compared with m19hBBz. **A,** CAR T-cell numbers with the indicated domains in the bone marrow (BM) over time *in vivo*. *Rag1*$^{-/-}$ mice were i.v. injected with 1 × 10^6 CAR T cells. After 1, 2, 4, or 6 weeks, femurs were removed, and CAR T cells were counted by flow cytometry. **B,** Donor T cells in the BM after antigen challenge after 1 week. One week after *Rag1*$^{-/-}$ mice were i.v. injected with 1 × 10^6 CAR T cells, mice were challenged with 1 × 10^6 Eμ-ALL cells. One week after challenge, donor T cells in the femur were counted by flow cytometry. **C-G,** *Rag1*$^{-/-}$ mice were i.v. injected with m19dz, m19z, m1928z, or m19hBBz 1 × 10^6 CAR T cells. After 5 weeks, mice were challenged with 1 × 10^6 Eμ-ALL cells. One week after antigen challenge, CART (**C**) and donor (**D**) cells in the femur were counted by flow cytometry. CAR T cells were also analyzed for memory T-cell phenotype (**E**), PD-1 (**F**), and LAG3 (**G**). Data are representative of two independent experiments. For **A-D**, each group has 4 mice. Error bars, SD. *, $P < 0.05$; **, $P < 0.01$ by one-way ANOVA.

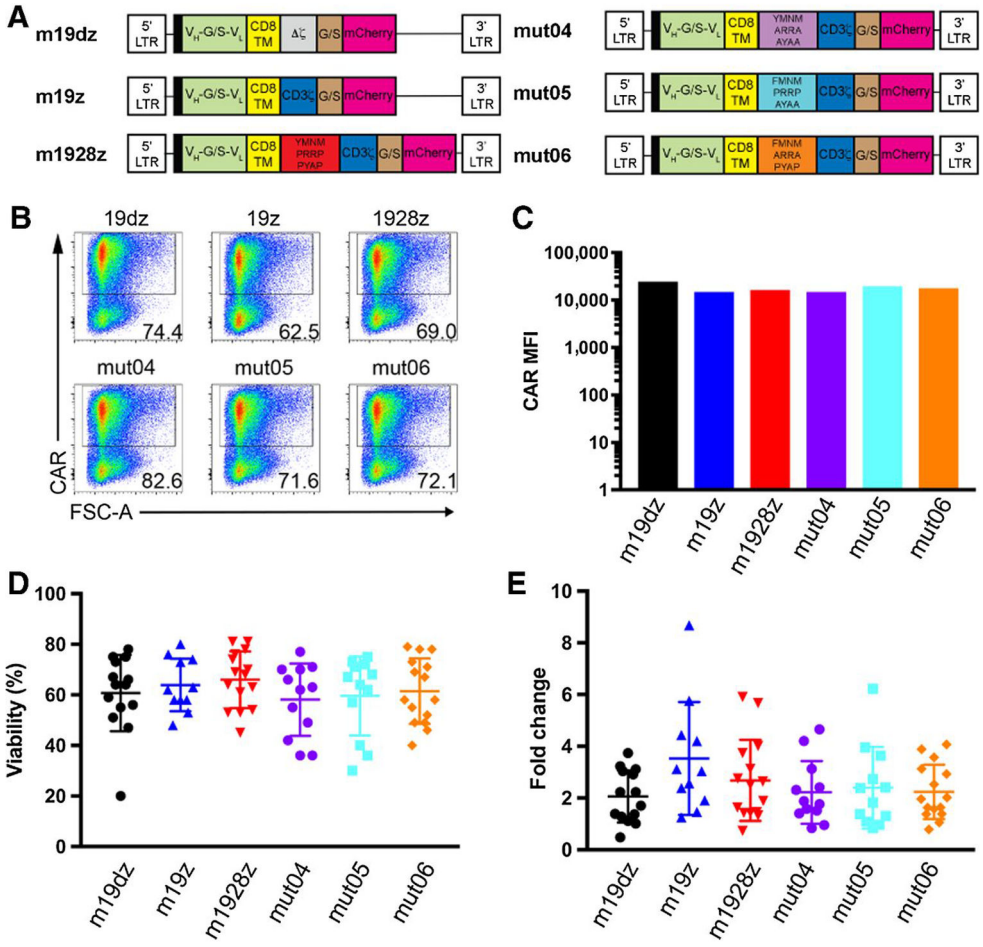

Figure 2.

CD28 mutant CAR characterization. **A,** Schematic of CAR constructs. All included a 5′ long terminal repeat (LTR), CD8 signal peptide (black bar), scFv with a variable heavy chain connected with glycine–serine linker to a variable light chain (V_H-G/S-V_L), CD8 transmembrane and hinge domain, costimulatory and/or CD3ζ endodomain, glycine–serine linker (G/S), mCherry reporter, and 3′ LTR (33). **B,** CD28 mutant CAR transduction efficiency. A representative flow plot of CAR expression. FSC-A, forward-scatter area. **C,** CAR MFIs measured by mCherry. **D** and **E,** CD28 mutant CAR T-cell viability (**D**) and proliferation (**E**) compared with nonmutated CD28 CAR T cells prior to antigen stimulation. CAR T cells were counted after day 5 of production with trypan blue to determine viability and proliferation. For **B** and **C**, data are representative of 11 independent experiments. For **D** and **E**, each data point represents one CAR production. Error bars, SD.

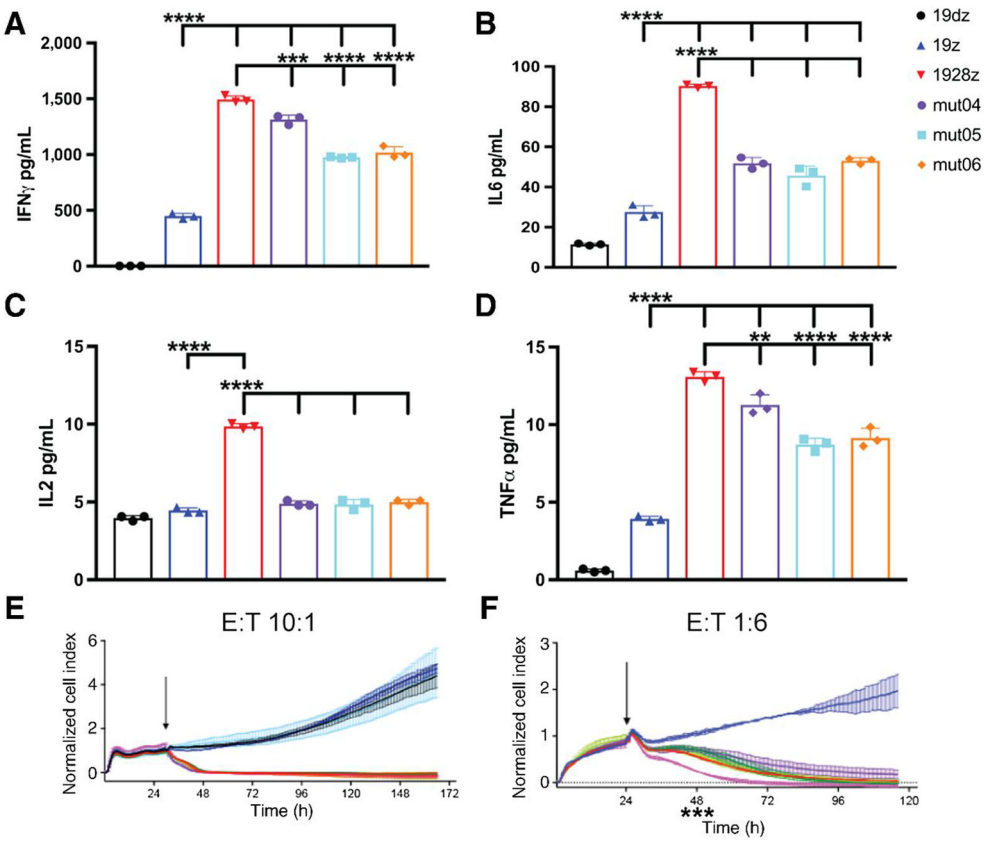

Figure 3.

CD28 mutant CAR T-cell *in vitro* function. **A-D,** Cytokine production of CD28 mutant CAR T cells compared with m1928z and m19z CAR T cells. CAR T cells were stimulated with 3T3-mCD19 cells at a 10:1 E:T ratio. After 24 hours, supernatants were harvested, and IFNγ (**A**), IL6 (**B**), IL2 (**C**), and TNFα (**D**) were measured by Luminex. **E** and **F,** Cytotoxicity of CD28 mutant CAR T cells compared with nonmutated CD28 CAR T cells. CAR T cells were cocultured with 3T3-mCD19 at either 10:1 (**E**) or 1:6 (**F**) E:T ratios. The xCelligence RTCA system monitored cytotoxicity. Arrows indicate the time point of CAR T-cell addition. Data are representative of three independent experiments. Error bars, SD. **, $P < 0.01$; ***, $P < 0.001$; ****, $P < 0.0001$ by one-way ANOVA.

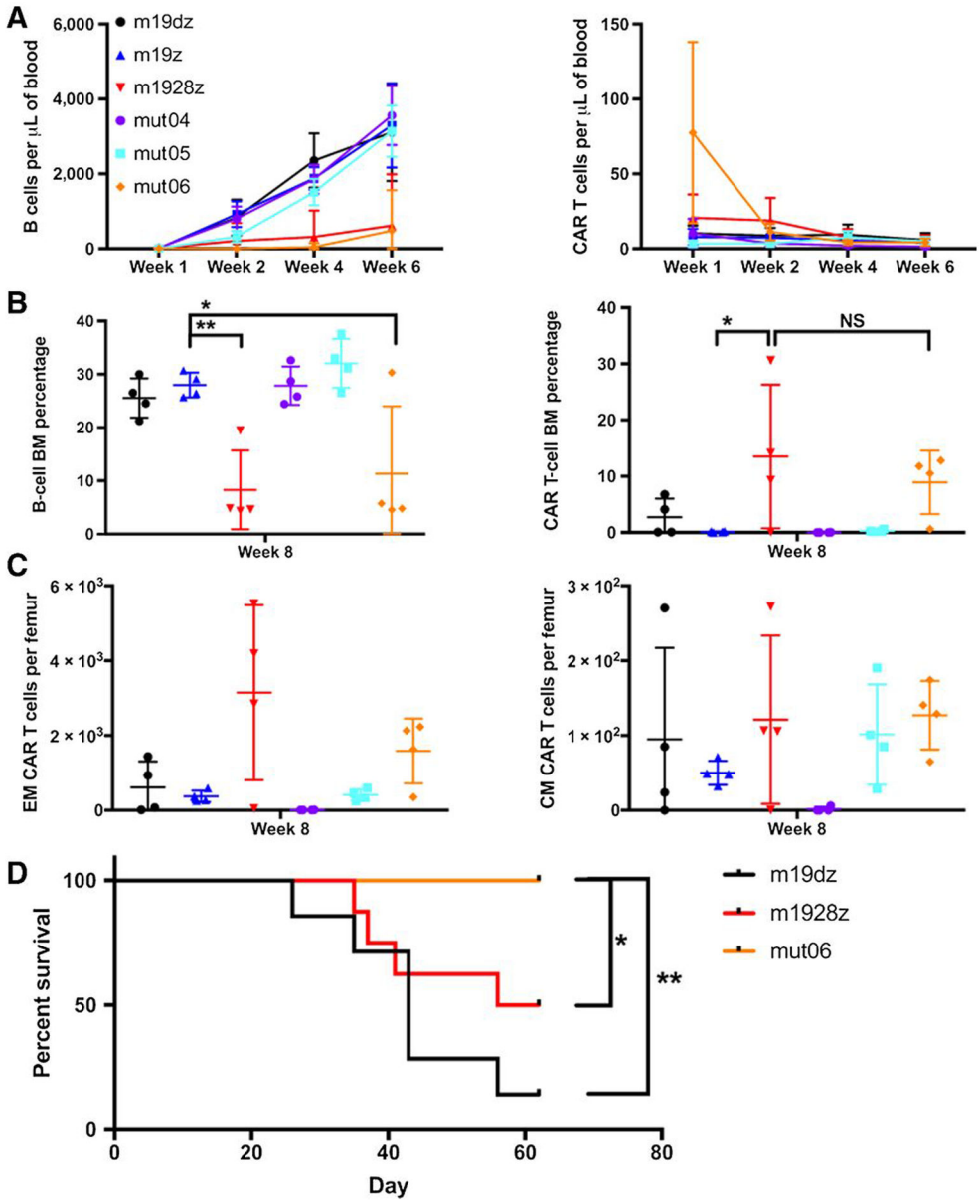

Figure 4.

Mut06 CAR T cells support optimized *in vivo* function. C57BL/6 mice were injected i.p. with cyclophosphamide (300 mg/kg) 1 day prior to i.v. injection of 3×10^5 CAR T cells. Blood and bone marrow (BM) were collected at indicated time points and analyzed by flow cytometry. **A,** B-cell and CAR T-cell counts in the blood in weeks 1 to 6. **B,** B-cell and CAR T-cell percentage in BM after 8 weeks. **C,** CD28 mutant and nonmutated CAR T cells have similar memory phenotype counts at week 8. **D,** Mice with mut06 CAR T cells have better survival after Eμ-ALL challenge compared with m1928z CAR T cells. C57BL/6 mice were i.v. injected with 1×10^6 Eμ-ALL cells. On day 6, mice were injected i.p. with 300 mg/kg of cyclophosphamide. On day 7, mice were i.v. injected with 3×10^5 CAR T cells. Mice were then sacrificed after a 20% loss of body weight according to the IACUC-approved protocol. For **A-C**, each group has four mice and is representative of two independent experiments.

For **D**, each group has eight mice. Error bars, SD. *, $P < 0.05$; **, $P < 0.01$ by one-way ANOVA.

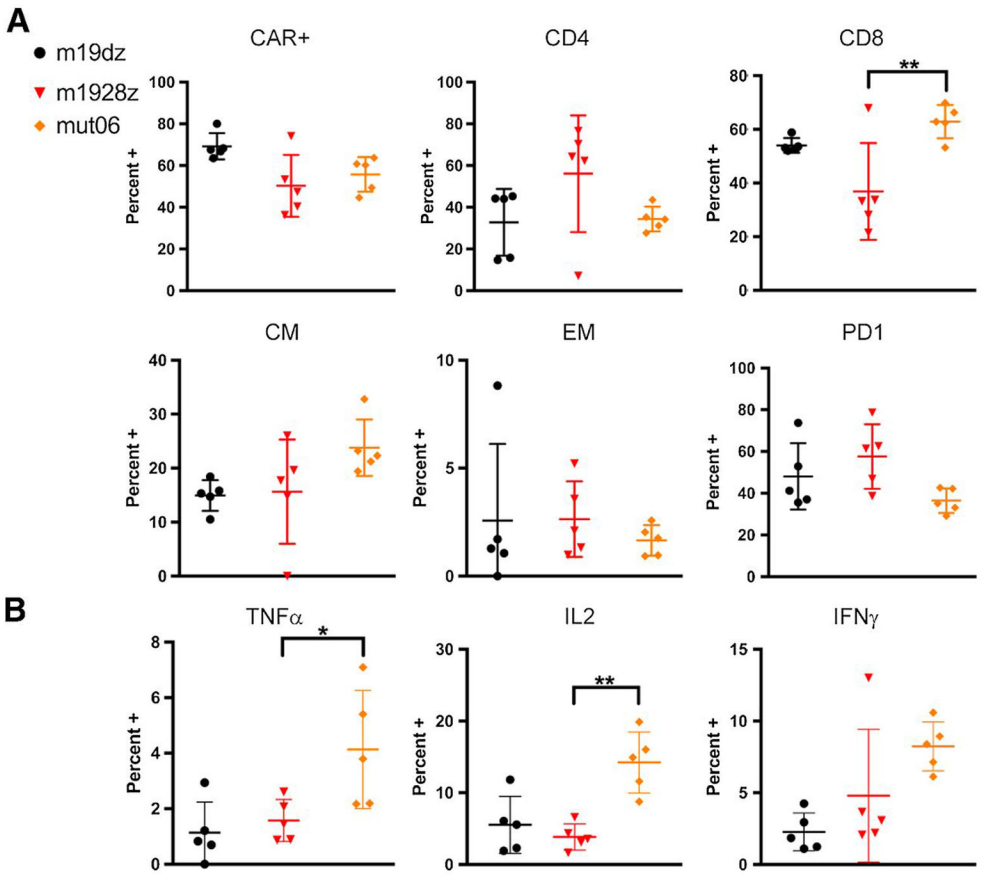

Figure 5.

Mut06 CAR T cells remain sensitive to antigen *in vivo*. CAR T-cell phenotype after antigen challenge *in vivo*. *Rag1*$^{-/-}$ mice were injected with 1 × 10^6 CAR T cells. After 1 week, mice were challenged with 1 × 10^6 Eμ-ALL antigen. Following 1 week of antigen challenge, mice were sacrificed, and bone marrow was collected. **A,** CAR T-cell phenotypes were determined using flow cytometry. **B,** Mut06 CAR T-cell cytokine expression compared with m1928z CAR T cells. Following 1 week of antigen challenge, mice were sacrificed and splenocytes were collected. Splenocytes were then cocultured with 3T3-mCD19/mPD-L1 in the presence of 1× protein transport inhibitor. After 4 hours, cells were stained for intracellular cytokines and analyzed by flow cytometry. Each group has five mice. Data are representative of two independent experiments. Error bars, SD. *, $P < 0.05$; **, $P < 0.01$ by one-way ANOVA.

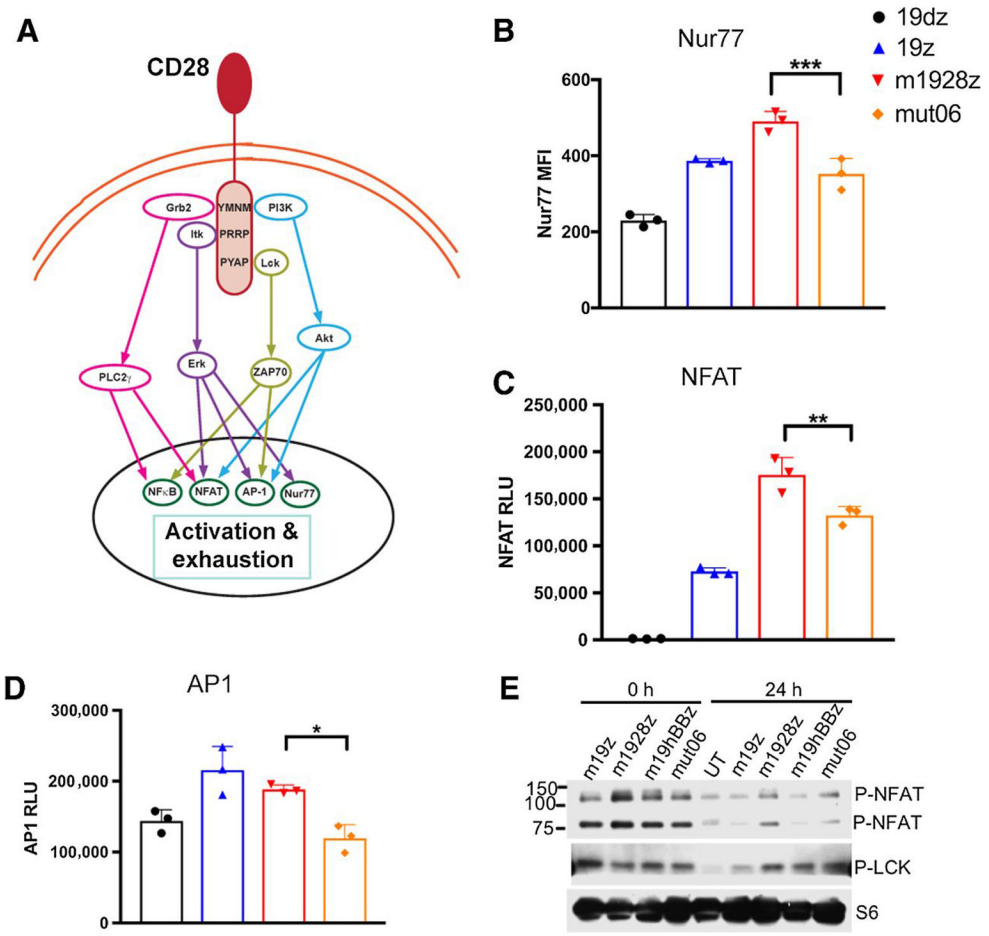

Figure 6.

Mut06 CAR T cells have decreased expression of exhaustion-related transcription factors. **A,** Schematic of CD28 signaling. **B,** Mut06 CAR T-cell Nur77 expression compared with m1928z CAR T cells. Spleens were harvested from Nur77^{GFP} mice, and T cells were isolated. CAR T cells were produced and stimulated for 24 hours with 3T3-mCD19 cells. GFP was measured by flow cytometry. NFAT (**C**) and AP1 (**D**) in mut06 CAR T cells compared with m1928z cells. Jurkat cells with NFAT or AP1 firefly luciferase reporters were transduced with CARs and stimulated with 3T3-mCD19 cells. After 24 hours, cells were lysed and supernatants were analyzed with a luminometer. **E,** Phospho(p)-NFAT in mut06 compared with m1928z CAR T cells. CAR T cells were stimulated for 24 hours by 3T3-mCD19 cells or immediately lysed for Western blot and probed for p-NFAT, p-LCK, and S6. **B-E,** Data are representative of three independent experiments. Error bars represent SD. *, $P < 0.05$; **, $P < 0.01$; ***, $P < 0.001$ by one-way ANOVA.

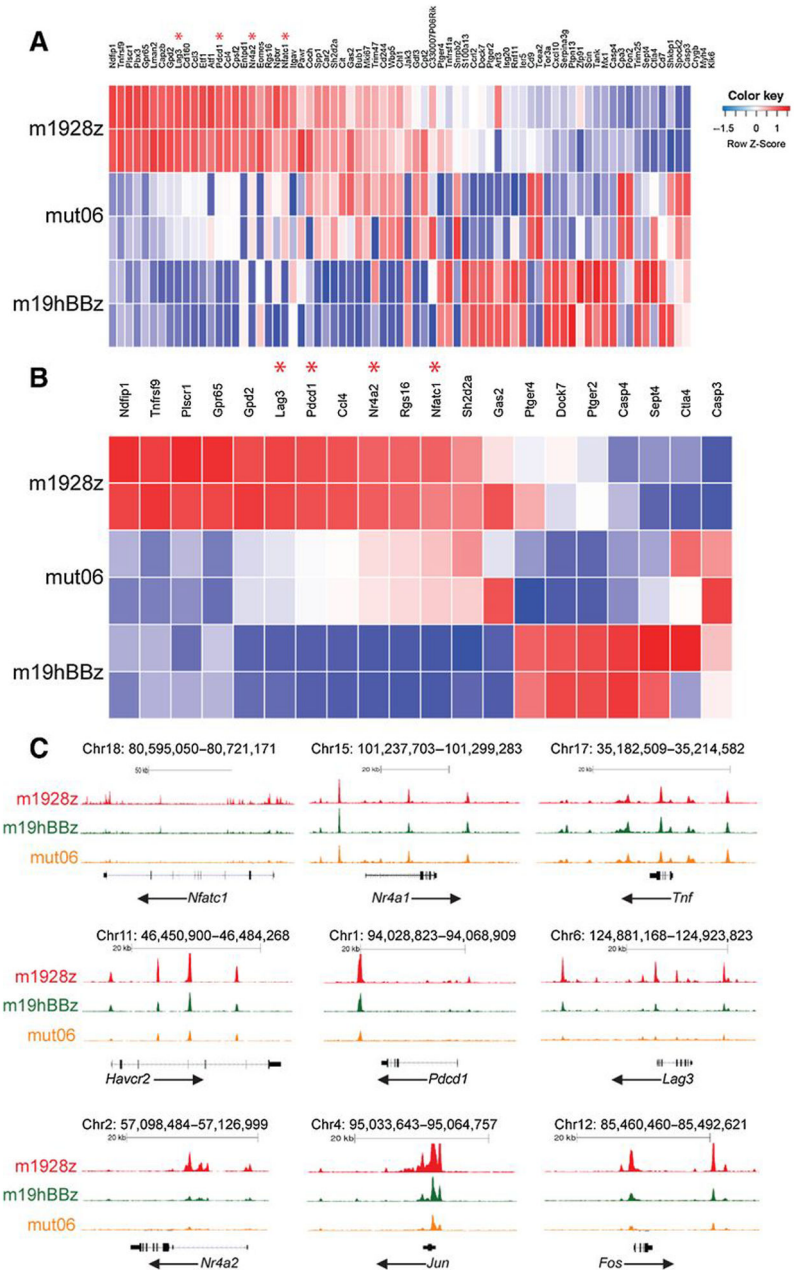

Figure 7.

Mut06 has less exhaustion-related gene expression and accessibility. **A,** RNA-seq heat map of 78 exhaustion-related T-cell genes. Cells were stimulated for 24 hours with 3T3-mCD19, and CAR T cells were sorted and lysed. RNA-seq was performed with 100-nt sequence reads using Illumina HiSeq 4000. **B,** RNA-seq heat map of 22 NFAT exhaustion-related T-cell genes (23, 33). **C,** Genome browser view of the *Nfatc1*, *Tnf*, *Havcr2*, *Pdcd1*, *Nr4a1 (Nur77)*, *Nr4a2*, *Lag3*, *Jun*, and *Fos* loci after ATAC-seq. Cells were stimulated for 24 hours with 3T3-mCD19, and CAR T cells were sorted and lysed. Paired-end 42-bp sequencing reads generated by Illumina sequencing using NextSeq 500 were mapped to the genome

using the BWA algorithm with default setting. Red stars denote the presence of the gene in ATAC-seq panel **C**.